β-decay study of neutron-rich bromine and krypton isotopes

K. Miernik *et al.*

Phys. Rev. C **88**, 014309 — Published 12 July 2013
DOI: 10.1103/PhysRevC.88.014309

Beta-decay study of neutron-rich isotopes of Bromine and Krypton

K. Miernik,[1,2,*] K.P. Rykaczewski,[1] R. Grzywacz,[3,1] C.J. Gross,[1] D.W. Stracener,[1] J.C. Batchelder,[4] N.T. Brewer,[5] L. Cartegni,[3] A. Fijałkowska,[2,3] J.H. Hamilton,[5] J.K. Hwang,[5] S.V. Ilyushkin,[6] C. Jost,[3] M. Karny,[2,4] A. Korgul,[2] W. Królas,[7] S.H. Liu,[4] M. Madurga,[3] C. Mazzocchi,[2] A.J. Mendez II,[1] D. Miller,[3] S.W. Padgett,[3] S.V. Paulauskas,[3] A.V. Ramayya,[5] R. Surman,[8] J.A. Winger,[6] M. Wolińska-Cichocka,[1,4,9] and E.F. Zganjar[10]

[1] *Physics Division, Oak Ridge National Laboratory, Oak Ridge Tennessee 37830 USA*
[2] *Faculty of Physics, University of Warsaw, Warsaw PL-00-681, Poland*
[3] *Dept. of Physics and Astronomy, University of Tennessee, Knoxville, Tennessee 37996, USA*
[4] *Oak Ridge Associated Universities, Oak Ridge, Tennessee 37831, USA*
[5] *Dept. of Physics and Astronomy, Vanderbilt University, Nashville, Tennessee 37235, USA*
[6] *Dept. of Physics and Astronomy, Mississippi State University, Mississippi, 39762, USA*
[7] *Institute of Nuclear Physics, Polish Academy of Sciences, Cracow PL-31-342, Poland*
[8] *Dept. of Physics and Astronomy, Union College, Schenectady, New York 12308, USA*
[9] *Heavy Ion Laboratory, University of Warsaw, Warsaw PL-02-093, Poland*
[10] *Dept. of Physics and Astronomy, Louisiana State University, Baton Rouge, Louisiana 70803, USA*

(Dated: June 24, 2013)

Short-lived neutron-rich nuclei including ^{93}Br, ^{93}Kr and ^{94}Kr were produced in proton-induced fission of ^{238}U at the HRIBF in Oak Ridge. Their beta decay was studied by means of a high resolution on-line mass separator and beta-gamma spectroscopy methods. The half-life of $T_{1/2} = 152(8)$ ms and β-delayed branching ratio of $P_n = 53^{+11}_{-8}\%$ measured for ^{93}Br differs from the previously reported values of $T_{1/2} = 102(10)$ ms and $P_n = 68(7)\%$. At the same time the half-life of ^{94}Kr $T_{1/2} = 227(14)$ ms and both half-life of $T_{1/2} = 1.298(54)$ s and β-delayed branching ratio of $P_n = 1.9^{+0.6}_{-0.2}\%$ of ^{93}Kr are in very good agreement with literature values. The decay properties of ^{93}Br include previously unreported gamma transitions following beta-delayed neutron emission.

I. INTRODUCTION

Decay probabilities are among the basic properties characterizing radioactive nuclei. Nuclear theories aim to describe known half-life values and predict decay properties of nuclei that are beyond experimental reach. Accurate experimental determinations of decay properties for exotic nuclei serve as anchor points for extrapolations into unknown nuclear territories.

The region around the Z = 40 and N = 56 sub-shell closures is rich in many interesting and surprising features. Depending on the small changes in nuclear structure, the neighboring nuclei might be significantly deformed or nearly spherical (e.g ^{96}Sr and ^{96}Kr [1]). As the interpretation of such phenomena often relies on the comparison of experimental data with theoretical calculation, the accurate knowledge of basic nuclear properties is important for studying the systematic behavior along isotonic or isobaric chains and for subsequent verification of theoretical analysis.

An additional motivation for measuring the decay rates of very neutron-rich nuclei is related to the analysis of the nucleosynthesis process. The nuclei studied in this work are expected to be involved in the rapid-neutron-capture process [2], and therefore their decay probabilities may affect the actual path as well as the post r-process abundances [3].

The region of neutron-rich Br and Kr isotopes is also important for nuclear reactor science. These isotopes are located close to the peak of the ^{235}U and ^{239}Pu fission yield distributions. Decay properties, in particular the half-life, decay heat, and beta-delayed neutron emission, contribute to the analysis of the post-fission processes in nuclear fuels [4]. The complex environment of a nuclear reactor led nuclear-cycle simulations to adopt a 6-group representation of the beta-delayed neutron emission from fission products [5, 6]. The βn precursors are assigned to groups according to their half-lives, where group 1 includes the longest and group 6 — the shortest. Thus the short-lived ^{93}Kr belongs to group 5 (half-lives 0.4—1.4 s). The ^{93}Br half-life and P_n were not included in the reference compilation [5]; however, they could be added to group 6 (half-lives < 0.4 s). It is worth noting that both of its decay daughters, ^{92,93}Kr, are included therein.

The β-decay scheme of ^{93}Br was previously reported in [7] while the half-life comes from an earlier report [8]. The β-delayed branching ratio was given in reference [8] as $P_n = 10(5)\%$ and later revised by the same group to 68(7)% [7]. The detailed discussion of differences in results between our value and that of previous work is presented in section III A.

II. EXPERIMENTAL TECHNIQUE

The experiment was performed at the Holifield Radioactive Ion Beam Facility (HRIBF) [9, 10] at Oak Ridge National Laboratory. A 50 MeV proton beam of average

* kmiernik@fuw.edu.pl

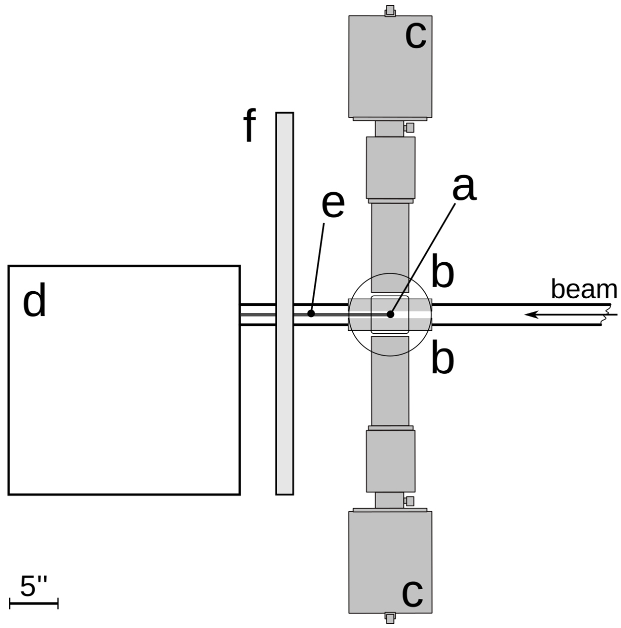

FIG. 1. Schematic view of the detector setup. The 200 keV ions are implanted in the middle (a) of the array of two β-counters (b) and four Ge clover detectors (c). Two of the clovers are placed in the plane perpendicular to the plane of the figure and are symbolized by the square and circle. Moving Tape Collector device (d) is operating the implantation tape (e) and is located behind the 2-inch-thick lead shielding (f).

intensity of 9 μA was used to induce fission in a UC_x target of 6 g/cm^2 thickness. For this experiment, the ion source on the new HRIBF IRIS2 high-voltage platform IRIS2 [10] was used. Radioactive ions were extracted with a single positive charge, mass analyzed by a low resolution magnet ($m/\Delta m \approx 1000$), accelerated to 200 keV and then further mass analyzed by a high resolution magnet ($m/\Delta m \approx 10000$). The separated ion beams of enhanced isobaric purity were then transmitted to the Low Energy Radioactive Ion Beam Spectroscopy Station (LeRIBSS)[10].

The LeRIBSS station was equipped with a Moving Tape Collector (MTC), four high purity Ge clover detectors, and two plastic β detectors surrounding the implantation point located inside a thin-walled vacuum chamber (Figure 1). The photo-peak efficiency for the clover array was 34% for γ-rays of 81 keV and 6% for 1.33 MeV γ rays. The β detectors were used to reduce background in the γ spectrum by requiring γ-β coincidences. The efficiency of the β counter is a function of the beta energy. The expected beta energy for a given gamma line can be described by the so-called effective Q value which is related to the feeding of a given level. The β efficiency is equal to about 20% for $Q_{\text{eff}} = 3$ MeV and 57% for $Q_{\text{eff}} = 6.7$ MeV. The details of establishing the β efficiency are given in reference [11].

The MTC was operated in "take-away" mode, a three-step cycle consisting of a period t_1 during which ions are implanted into the magnetic layer of a 3M Blackwatch 700 tape, a decay measurement period t_2 during which the ion beam is deflected into a beam dump by an electrostatic kicker, and finally a tape-transport period t_3 during which the irradiated spot on the tape is moved 18" into a two-inch-thick-lead-shielded tape chamber. For this work, the measurement was performed over an 8-hour period using a 1 s - 1 s - 425 ms cycle. An additional measurement lasting 1.5 h using a 1 s - 4 s - 425 ms cycle was also performed.

The germanium clover detectors, the beta counters, and the MTC control signals were read by the XIA Pixie16 Rev. D digital electronics modules [12]. The acquisition system was operated without a master trigger, and all events above the noise threshold were recorded independently and time-stamped with a 100 MHz clock synchronized across all modules. The coincidence gates and clover add-back corrections were applied on the software level and could be adjusted during off-line analysis. In the range of count rates observed in this experiment (approximately 1 kHz / channel) the system is practically dead-time free [13, 14].

III. RESULTS AND DISCUSSION

A. β-decay of ^{93}Br

Figure 2 shows the β-gated γ-spectrum measured during our experiment. The energy spectrum was recorded up to 8.2 MeV. However, since no γ-transitions above 1 MeV were assigned to the decay of ^{93}Br, only the low-energy region is shown. All of the γ-lines observed in the spectrum were identified. The beam composition included only ^{93}Br, ^{93}Kr and ^{93}Rb. The ^{93}Sr and ^{93}Y γ-rays that appeared were result of transport tape contamination with previous implantation spots. The time to fully use the tape loop was about 30 minutes. Since the half-lives of ^{93}Sr and ^{93}Y is 7.4 min and 10 h ,respectively, those activities are accumulated following the decay of other isotopes in the A = 93 isobaric chain. As expected, the intensities of ^{93}Sr and ^{93}Y do not reveal a grow-in/decay pattern characteristic of other short-lived activities, but they are constant in time and easily recognizable.

The most exotic isotope in the chain is ^{93}Br. Thus, its activity relative to the cycle time can be described by the simple relations:

$$f(t) = \begin{cases} P(1 - e^{(-t/\tau)}) & t_1 > t > 0 \\ P(1 - e^{(-t_1/\tau)})e^{(-t/\tau)} & t_2 > t > t_1 \end{cases} . \quad (1)$$

The parameter P is a product of the ion flux per second (Φ), the branching ratio for a given line (I_γ), and the detector system efficiencies (ε_γ, ε_β), $P = \Phi I_\gamma \varepsilon_\gamma \varepsilon_\beta$. Since all those values are constant during the implantation period of the cycle, P is not decomposed in the analysis,

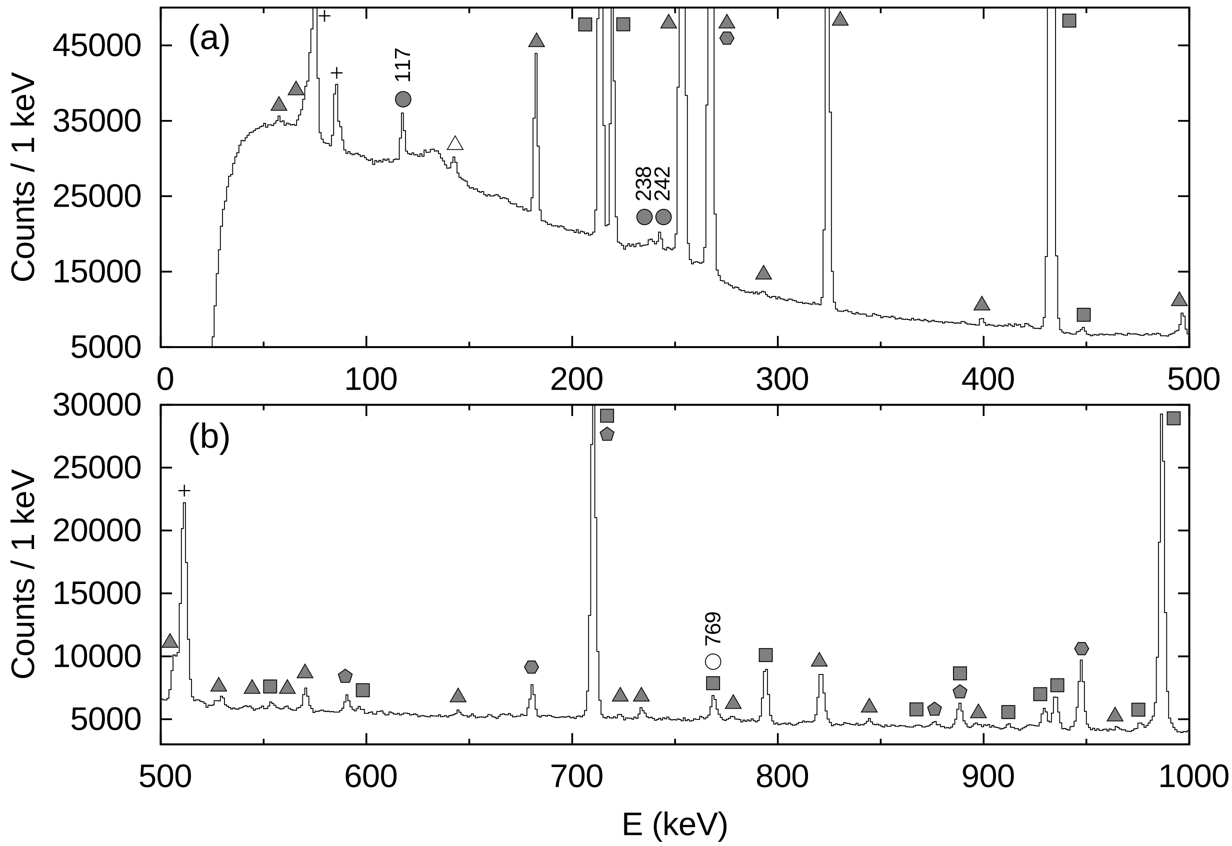

FIG. 2. Beta-gated γ-ray spectrum for mass A = 93. Transitions are marked by parent decay: circles (^{93}Br), triangles (^{93}Kr), squares (^{93}Rb), pentagons (^{93}Sr), hexagons (^{93}Y) and crosses (background transitions). Filled symbols indicate β decay, while open symbols indicate that the transition is due to β-delayed neutron emission.

and it is treated as a fit parameter along with the mean life-time (τ). Times t_1 and t_2 are the ends of the grow-in part of the cycle and the entire cycle, respectively. The values of t_1 and t_2 were set and measured with 1 ms precision.

The half-life value of ^{93}Br was determined by analysis of the decay patterns of the 117, 238, 242 and 769 keV γ-rays. In all cases, a gate on the γ-ray energy was set in the energy-versus-cycle-time spectrum. The background was subtracted by placing a gate in the region close to the γ-line. The background gate was always selected symmetrically in the energy spectrum, with an equal number of channels left and right of the γ-line. The background gate had in total the same number of channels as the γ gate. Equation 1 was fit to experimental points with a non-linear least-squares algorithm using Numerical Python [15] and Lmfit libraries [16]. The correctness of the fit was confirmed by changing background gates as well as by choosing different minimalization algorithms and comparing the results. Additionally, a fit only to the decay part of the cycle was also performed. The distribution of fit results using various gates and methods was within one standard deviation of statistical uncertainty of the best fit parameters. The analysis of the decay pattern for the 117 keV transition yields $T_{1/2}(^{93}\mathrm{Br})$ = 155(10) ms and is presented in Fig. 3.

An initial half-life fit for the 769 keV transition yielded 188(16) ms. However, this line included a weak 768.4 keV line ($I_\gamma = 0.133\%$) from the decay of ^{93}Rb [17]. Since the decay of this isotope is well known [17, 18], one can subtract this contribution by analyzing the relative intensity of other ^{93}Rb lines. The intensity of this contamination contributes 22.8 % of the total number of counts in the 769 keV line. The resulting fit, with ^{93}Rb contamination subtracted, yields $T_{1/2} = 144(14)$ ms and is presented in Fig. 3.

The 152(8) ms measured half-life value of $T_{1/2}(^{93}\mathrm{Br})$ is a weighted average of half-lives found for the 117, 238, 242 and 769 keV lines. The internal and external uncertainty of ± 7 and ± 8 ms, respectively, were found to be consistent, indicating the correct assignment of these lines to the decay of the same parent.

The half-life of ^{93}Br was previously given as 102(10) ms in [8]. Transitions assigned to ^{93}Br decay and a partial decay scheme were later reported in [7]. The half-life of 102(10) ms differs by more than 3σ from the value of 152(8) ms found in this work. Recently, the half-life of ^{93}Br was measured in a heavy-ion fragmentation experiment [19]. However, the accuracy of the result 69^{+40}_{-25} ms is limited by the very small statistics of only 20 recorded

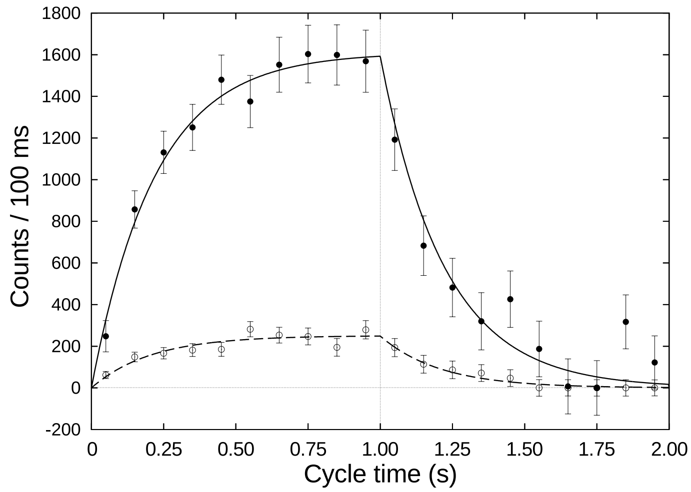

FIG. 3. Decay half-life measurement for ^{93}Br determined by the 117 keV and 769 keV transitions. The experimental points (background-subtracted) are shown with a filled (117 keV) and open circles (769 keV). The result of the fit is shown with a solid (117 keV) and dashed lines (769 keV).

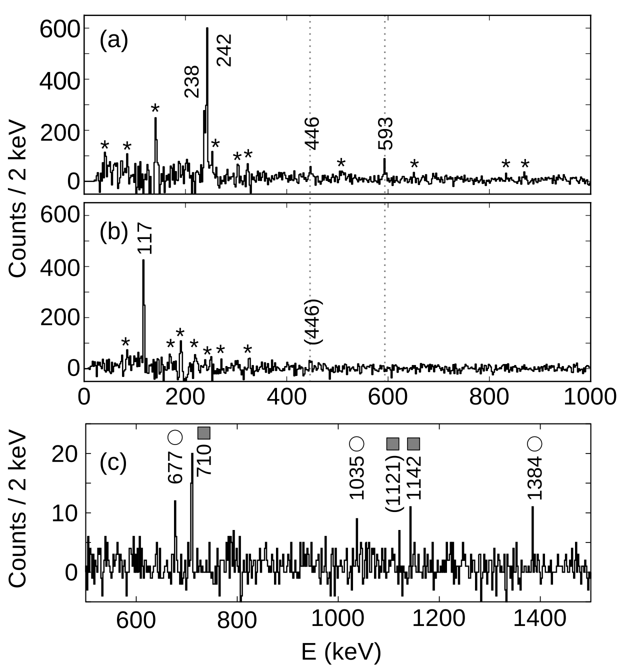

FIG. 4. Background subtracted γ-γ coincidence spectra gated on the following transitions: 117 keV (a), 242 keV (b) and 769 keV (c). The peaks marked with star ($\star$) are artifacts due to the background subtraction procedure. The peaks marked with numbers are transitions in ^{93}Kr (no symbol), ^{92}Kr (circles) and ^{93}Rb (squares).

ion-beta correlated events. No gamma radiation characteristic for ^{93}Br decay could be observed in the latter experiment [19]. The source of the discrepancies in half-life between the present and previous work is unclear due to the lack of supporting evidence such as spectra and decay curves in [8].

The two lowest excited levels at 117 keV and 354 keV in ^{93}Kr were seen after high spin states were populated in spontaneous fission of ^{252}Cf [20]. The reported 10 ns half-life for the 354 keV state indicates presumably an E2 transition and tentative spin assignment $3/2^{+}$ and $7/2^{+}$ for the first two states.

In our study, the gamma lines were assigned to the decay of ^{93}Br by their characteristic half-life and by coincidence with established lines. The procedure of obtaining γ-γ spectra included symmetrical background subtraction similar to the one used in the half-life analysis. In the coincidence spectra, we observed so called cross-talk peaks originating from Compton scattered γ-rays recorded by the neighboring clover crystals. These artificial peaks might be of comparable intensity to real coincidences for strong lines from long-lived contaminants. In order to exclude such peaks from the analysis, we compared γ-γ spectra recorded during the first and last 500 ms of the decay part of cycle. Only those peaks that were present in the first spectrum and not present in the second one were taken into account. This procedure was especially important for the 593 keV line found in the $\gamma-\gamma$ spectrum gated on the 117 keV line. The intensity of the 593 keV line had to be corrected for cross-talk events originating from the 710.3 keV line found in the decay of ^{93}Rb. An example of the γ-γ spectra is shown in Fig. 4.

We have observed clear coincidences between 117 keV and the 238, 242, 446 and 593 keV lines. The 446 keV line was also possibly observed in coincidence with 242 keV. The gate set on 769 keV line, assigned to ^{92}Kr [21], shows three other γ-transitions known from spontaneous fission fragments of ^{248}Cm [22]. In addition, lines in coincidence with the weak 768.4 keV ^{93}Rb line contamination are visible.

The coincidence data were used to build the partial decay scheme presented in Fig. 5. A conversion coefficient for the 117 keV transition, $\alpha_K = 0.058(10)$ [7], is included in the presented decay scheme. The apparent beta feeding shown is deducted from the scheme. Table II presents a more detailed summary of γ-transitions assigned to the decay of ^{93}Br. All intensities are corrected for summing effects [23] using the experimental decay scheme information.

We were not able to confirm the 710.3 keV transition in ^{93}Kr reported in [7] because this energy region was dominated by a strong 709.95 keV line from ^{93}Rb decay. The transitions at 349.9, 669.5, 966.4, 977.6, and 1142 keV reported in [7] as coincident with the 117 keV and 242 keV lines, as well as unplaced transitions in the decay scheme of energies above 2 MeV, were also not observed in our experiment.

The decay scheme presented in Fig. 5 includes for the first time β-delayed neutron branchings to the excited states in ^{92}Kr [20, 22]. It is especially surprising that they were not reported by Lherssoneu et al. [7], since the β-delayed branching ratio given in that work $P_n = 68(7)$ % suggest that this is the main decay path of ^{93}Br. The

TABLE I.

TABLE II. Summary of γ lines assigned to the decay of ^{93}Br. Intensity is relative to the strongest transition observed in a given nucleus.

Energy (keV)	I_γ	$T_{1/2}$ (ms)	$\gamma - \gamma$
β-decay			
117.5(2)	100(6)	155(10)	238, 242, (350), (446), 593
237.6(2)	33(6)	202(38)	117
242.5(2)	54(6)	130(40)	117, (446)
446.3(5)[a]	8(3)	—	117, (242)
593.4(5)[a]	17(4)	—	117
βn			
768.8(2)	100(6)	144(14)	677, 1035, 1384
677(1)[a]	3(1)	—	769
1035(1)[a]	2(1)	—	769
1384(1)[a]	4(1)	—	769

[a] Observed in coincidence spectra only.

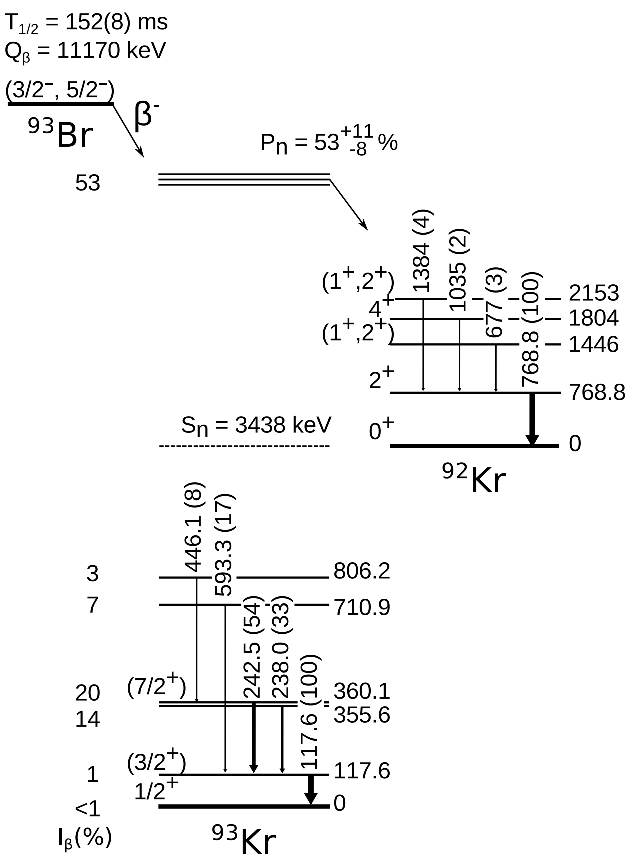

FIG. 5. Experimental decay scheme of ^{93}Br is shown (not drawn to scale). Q_β and S_n are taken from [24]. The spin assignment follows [1, 20, 22]. Other values are from this work.

cited P_n measurement was based on a comparison of intensities of γ transitions in the decay of the ^{93}Br β and β-n daughters. However, no details of the analysis were presented, nor was the reason given for the large discrepancy with the previously reported [8] $P_n = 10(5)\%$.

The ground state of ^{93}Br is not known, but spins of either $3/2^-$ or $5/2^-$, have been proposed presumably coming from an unpaired proton in the $p_{3/2}$ or $f_{5/2}$ orbitals. The observation of the 4^+ state in ^{92}Kr favors the ground state spin assignment of $5/2^-$. The lowest possible angular momentum barrier for the neutron is then L = 1 ($5/2^- \to 7/2^- \to 4^+$). If the ^{93}Br ground state is $3/2^-$, then the lowest angular momentum barrier is L = 3 ($3/2^- \to 5/2^- \to 4^+$), and the transition would be hindered. However, the 4^+ state could also appear due to de-excitation of some higher lying states, through undetected weak γ transitions. Therefore the $5/2^-$ ^{93}Br ground state spin assignment is tentative.

The observation of γ transitions in the β-n daughter gives us the opportunity to determine experimentally the β-delayed branching ratio (P_n) of ^{93}Br by comparing intensities of γ transitions in ^{93}Kr and ^{92}Kr.

The relations for P_n are

$$R = \frac{N(117)\varepsilon_\gamma(769)I_n(769)}{N(769)\varepsilon_\gamma(117)I_n(117)}$$

$$P_n = \frac{1}{1+R} \tag{2}$$

where N is the number of counts in the selected γ-ray transitions, ε_γ is the γ-ray detection efficiency, and I_n is the γ-ray intensity normalized per 100 decays leading to the given daughter nucleus.

The number of counts and detection efficiencies are measured. The procedure for determining the intensities will be discussed below. Since the decay scheme is clearly incomplete, the intensities must be found based on theoretical calculations. The calculations must include feeding to the ground state as well as unobserved transitions to higher energy states. The method we used is similar to the Cascading Gamma Model (CGM) developed by Kawano et al. [25] and successfully applied to calculate delayed neutron spectra [26].

a. ^{93}Kr ground state feeding The ground state spin $1/2^+$ of ^{93}Kr is known from laser spectroscopy[1]. If the ground state of ^{93}Br is $3/2^-$ the transition to the ground state of ^{93}Kr is a Gamow-Teller first forbidden transition. For this type of transition in odd-A isotopes the average $\log(ft)$ value is 7.3±1.0 and would result in I_β between 3.8 and 0.04% [27]. In the case of $5/2^-$ the transition to the ground state of ^{93}Kr is of first forbidden unique type with expected $\log(ft)$ values of 9.5±0.8, resulting in $I_\beta < 0.03\%$ [27]. In our calculations we have taken into account an average feeding to the ground state of 1%.

b. ^{93}Kr excited states feeding In order to take into account possible unobserved feeding to higher energy states de-exciting directly to the ground state, we used the well-studied decay scheme of the ^{93}Br isotone — ^{95}Rb [28]. The decay scheme was limited in energy to the ^{93}Kr neutron separation energy. The beta feeding was renormalized and the intensity of the lowest line (352 keV) was found to be 64 % per β0n branch. The decay scheme of ^{93}Br as presented by Lhersonneau [7] suggests the intensity of the lowest line (117 keV) to be 84 %. For calculation, we adopted an average $I_n(117) = 74(10)$ %.

c. ^{92}*Kr states feeding* To estimate the probability of transitions to the states in ^{92}Kr, we assumed that all neutron emission is following β transitions to the Gamow-Teller resonance (see Fig. 6). The position of the resonance was calculated using (p,n) reaction data systematics [29]. The distribution of feeding was calculated using Gross Theory [30] with a Gaussian distribution of probability with the standard parameter set of $\sigma_N = 6$ MeV and a Fermi level energy based on the Fermi gas approximation.

We assumed that the Gamow-Teller resonance splits into $1/2, 3/2, 5/2^-$ states if the ground state of ^{93}Br is $3/2^-$ and $3/2, 5/2, 7/2^-$ if it is $5/2^-$. The relative intensity of each spin I assumption was calculated from the formula

$$w(I, I_0) = \frac{2I+1}{3(2I_0+1)}, \tag{3}$$

where I_0 is the ^{93}Br ground state spin. For each known state in ^{92}Kr the neutron transmission probability was calculated taking into account the neutron energy and the angular momentum barrier found from the difference between the spins of the initial and final states. Transition probabilities were folded with the Gross Theory distribution to obtain relative level feedings. Using the known de-excitation paths of states in ^{92}Kr we subsequently found the normalized intensity of the 769 keV line to be 71 % in the case of ^{93}Br ground state $3/2^-$ and 76 % in the $5/2^-$ case.

By using Eq. 2 one can now calculate the β-delayed neutron emission probability. The resulting value is $P_n = 53\ ^{+11}_{-8}$ %, where the uncertainty includes a factor connected with the unknown ^{93}Br ground state spin assignment.

We have tested this method of P_n calculation by performing the calculations for ^{93}Kr decay, using the 142 keV line observed after β-delayed neutron emission and the 253 keV line found after β decay. In this case the well-studied excited states in ^{92,93}Rb were used as input data. The result of $P_n = 1.9^{+0.6}_{-0.2}$ % is in very good agreement with the adopted value of 1.95(5) %.

It must be noted that the model used in these calculations is limited to the cases where statistical treatment of the strength function in the β-decay is a reasonable approximation. In the case of the decay of ^{93}Br and ^{93}Kr, the window for neutron emission is large: $Q_\beta - S_n = 7.7$ MeV. Therefore, threshold effects are of small importance. Both β-daughter nuclei are odd-even as well as deformed (β_2 of ^{93}Kr is at the level of $0.2 - 0.3$

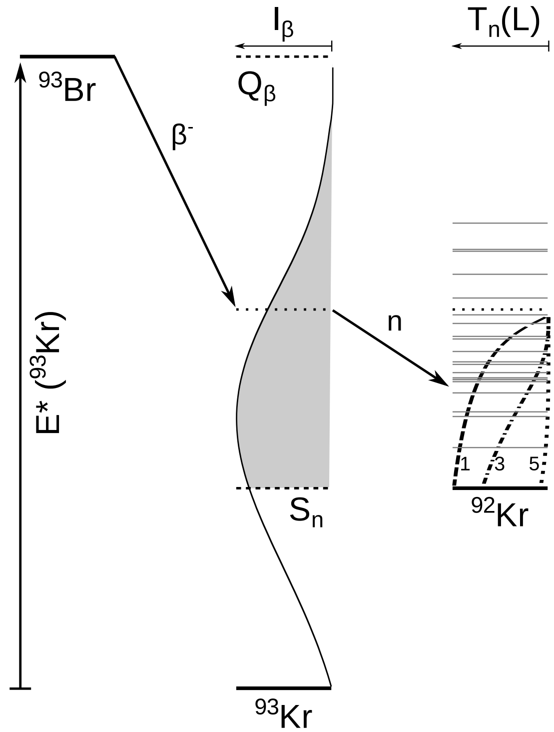

FIG. 6. Schematic representation of the method used to calculate the feeding of ^{92}Kr states populated after β-delayed neutron emission. The solid black line represents the feeding of states in ^{93}Kr calculated from the Gross Theory[30]. For a given excitation energy E^* the neutron transmission $T_n(L)$ probabilities were found (shown by dashed lines for l = 1, 3, 5) for each state in the ^{92}Kr (see text for more details).

[1]), which results in high level densities, and therefore the use of the simplified statistical model is justified.

B. Half-life of ^{93,94}Kr

Although the main goal of this experiment was to measure the decay properties of ^{93}Br, we have also analyzed the decay curves of ^{93,94}Kr in order to check our half-life determination method for possible systematic errors. Data for ^{94}Kr decay were analyzed with the same tape cycle as ^{93}Br. Data for the longer lived ^{93}Kr were analyzed with a 1 s – 4 s grow-in/decay cycle.

The adopted [18] value of ^{93}Kr half-life of $T_{1/2} = 1.286(10)$ s is a weighted average of three independent measurements [31–33]. Other values found in the literature are 1.17(4) s [34], 1.20(10) s [35], 1.29(1) s [36] and 1.04(10) s [19].

The most precise ^{94}Kr half-life measurement found in literature yields $T_{1/2} = 212(5)$ ms [37]. Other reported values are 210(10) ms [35], 220(20) ms [32], 330(100) ms [38] and 282(30) ms [19]. A weighted average of these results is 214(6) ms.

Figure 7 presents our analysis of the ^{93}Kr half-life. The result of the fitted function described by Eq. 1 is shown

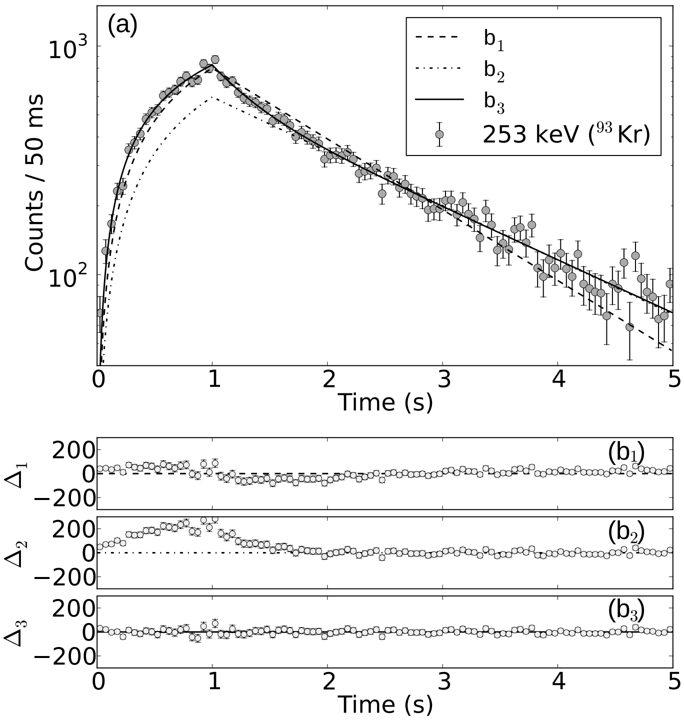

FIG. 7. Decay half-life measurement of ^{93}Kr. The background-subtracted experimental points for the 253 keV line are shown with filled circles. The fitted functions are shown with dashed, dashed-dotted and solid line. The respective residuals of the fits are shown in panels b_1 to b_3.

with a dashed line. The half-life of $T_{1/2} = 0.972(21)$ s is in disagreement with the adopted value. The residuals of this fit are presented in Fig. 7b$_1$. Clearly, an excess of counts in the first part of the cycle is seen, as well as a systematical shortage of counts in the region between 1.5 and 3.0 s.

The same function (Eq. 1) was used for the fit presented with a dashed-dotted line. However, only the points recorded between 2.0 and 5.0 s of the cycle were used and the function was subsequently extrapolated in the 0 - 2.0 s region. The result of this fit yields 1.267(42) s – in good agreement with literature values. The residuals shown in Fig.7b$_2$ reveal an excess of counts in the extrapolated region with a characteristic grow-in/decay pattern. This behaviour of residuals suggest that either an unknown β-decaying isomer exists in ^{93}Kr, or there is a physical effect that results in a loss of Kr atoms. Since we did not find any supporting evidence for the isomeric decay, we believe that this feature is a result of the diffusion of krypton atoms from the implantation tape.

The problem of diffusion of noble gases was discussed in several articles e.g. [37, 39] for He, Ne, Kr and Xe atoms. A very comprehensive discussion presented by Bergmann et al. [37] shows that a simple assumption that all atoms are diffusible is not sufficient. Instead, only some of the implanted atoms are escaping, while other remain trapped in the material. The diffusion process depends on many conditions during the experiment such as the chemical properties of the implanted atoms, the type of implantation material, the implantation energy of the atoms, the temperature of the system and the total implantation rate.

We assumed that atoms prone to diffusion are characterized by an effective mean half-life $\tau_{\rm eff}$, which fulfils the following equation:

$$\tau_{\rm eff} = \frac{\tau_\beta \tau_d}{\tau_\beta + \tau_d}, \tag{4}$$

where τ_β is the mean half-life of the β-decay and τ_d is the mean time for Kr atoms to escape from the material. The atoms from the second (non-diffusible) group are described by mean half-life of τ_β.

The function used to fit the data, takes the following form

$$f_d(t) = \begin{cases} PR(1-e^{(-t/\tau_{\rm eff})}) + P(1-R)(1-e^{(-t/\tau_\beta)}) & t_1 > t > 0 \\ PR(1-e^{(-t_1/\tau_{\rm eff})})e^{(-t/\tau_{\rm eff})} + P(1-R)(1-e^{(-t_1/\tau_\beta)})e^{(-t/\tau_\beta)} & t_2 > t > t_1 \end{cases}, \tag{5}$$

where P, t_1 and t_2 has the same meaning as in Eq. 1 and R is the ratio of number trapped atoms to the total number of atoms. As a result of the fit we obtained a half-life for ^{93}Kr of $T_{1/2} = 1.298(54)$ s and krypton diffusion half-life of $T^d_{1/2} = 0.295(68)$ s. The ratio of trapped atoms is $R = 0.16(2)$. The result of this fit is shown in the Fig. 7 by the solid line, and residuals are in the Fig. 7b$_3$.

In ref. [37] the reported diffusion half-life for $^{94-96}$Kr atoms was in range of 50–110 ms, and the percentage of diffusible atoms was 13–22 %. The larger diffusion half-life we see is most probably due to the higher implantation energy of 200 keV used in our experiment as compared to the 60 keV of the ISOLDE separator. The number of trapped atoms is presumably connected with the type of implantation material. The tape used in our experiment is built on mylar backing, as is the one in the setup of Ref. [37].

The diffusion parameters obtained in the measurement of ^{93}Kr were used in the half-life analysis of ^{94}Kr. The statistical level in this case was not sufficient to determine directly, with reasonable accuracy, the parameters of Eq. 5. We used γ-rays of 187, 220 and 629 keV to determine

TABLE III.

TABLE IV. Decay half-life measurements of ^{94}Kr, the non-corrected ($T^n_{1/2}$) and corrected ($T^d_{1/2}$) for the diffusion effect half-lives are presented.

Energy (keV)	$T^n_{1/2}$ (ms)	$T^d_{1/2}$ (ms)
187	222(29)	229(37)
220	214(16)	233(21)
629	215(17)	220(21)

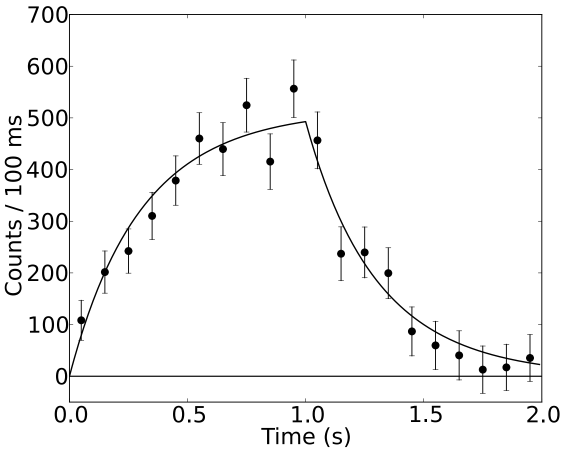

FIG. 8. Decay half-life measurement of ^{94}Kr. The background-subtracted experimental points for the 220 keV transition are shown. The result of the fit of function Eq. 5, which includes the paremeters of Krypton diffusion out of the tape, is shown with a solid line.

the half-life, and the results are presented in the table IV. The diffusion effect in this case is less pronounced since the diffusion half-life is longer than the β half-life, and both corrected and non-corrected results are within one standard deviation. A weighted average of the three diffusion-corrected results yields $T_{1/2} = 227(14)$ ms, in very good agreement with the literature value.

IV. COMPARISON OF RESULTS WITH THEORETICAL CALCULATIONS

Figure 9 presents a comparison of the ^{93}Br half-life and β-delayed neutron branching ratio from this experiment with the previously reported value [7], the various theoretical calculations: modified Gross Theory [40], FRDM+QRPA[41, 42], DF3a+CQRPA[43], and systematics [44]. Although none of the models can predict the observed values, the new experimental point seems to fit an expected systematic trend in the correlation between P_n and $T_{1/2}$ seen in the theoretical calculations.

All models are or were used for astrophysical r-process calculations. In order to analyze r-process abundances,

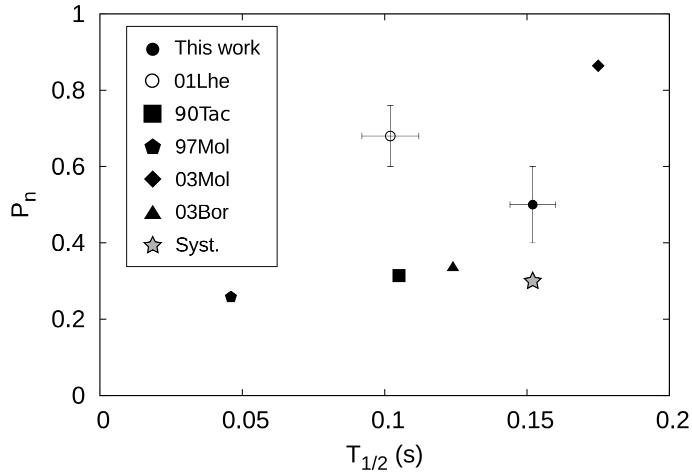

FIG. 9. Comparison of the experimental (this work and 01Lhe [7]) and theoretical (90Tac [40], 97Mol [41], 03Mol [42], and 03Bor [43]) ^{93}Br half-life and neutron branching ratio. The P_n value calculated using new systematics [44] based on experimental $Q_{\beta n}$ and $T_{1/2}$ is marked with a star.

both the half-lives and P_n values are very important [2, 3]. The half-lives affect the speed, path and range of nuclei created during the r-process, while P_n affects the resulting mass abundances. As ^{93}Br is located far from closed shells, it is expected that the new experimental half-life value will affect only the local mass (A = 92 – 94) abundance pattern. To verify this effect, calculations assuming a weak r-process scenario [3, 45] were performed. The analysis took into account the half-life and β-delayed neutron branching ratio predictions from [42] to obtain the reference abundances. Inclusion of the new experimental $T_{1/2}$ and P_n values for ^{93}Br resulted in local abundance differences for the A = 92–94 mass region at the 20% level.

V. SUMMARY

We have presented new results of β-decay studies of two neutron-rich A = 93 isobars, ^{93}Br and ^{93}Kr. The measurements were performed using mass-separated, fission-fragment beams of enhanced isobaric purity and a state-of-the-art detector setup with digital electronics. The revised beta half-life value of 152(8) ms for ^{93}Br differs from the accepted [18] value by more than 3σ. The isobaric selectivity of the experiment together with the trigger-less acquisition system allowed for detailed analysis of the data. The measured decay modes, including half-lives and β-delayed neutron emission, for the A = 93 isobaric chain are of importance not only for astrophysical models, but also are included in the irradiated nuclear fuel inventory calculations [4]. Global models were not able to reproduce the half-life and β-delayed neutron branching ratios. The best input values for nuclear network calculations, like r-process, modeling come from experimental observations, which are also needed for further development and verification of theoretical modeling.

ACKNOWLEDGMENTS

We would like to thank the HRIBF operations staff for the production of excellent radioactive ion beams.

K. Miernik's research was performed as a Eugene P. Wigner Fellow and staff member at the Oak Ridge National Laboratory, managed by UT-Battelle, LLC, for the U.S. Department of Energy under Contract DE-AC05-00OR22725. This research is sponsored by the Office of Nuclear Physics, U. S. Department of Energy under contracts DE-AC05-00OR22725 (ORNL), DE-FG02-96ER40983 (UTK), and DE-AC05-06OR23100(ORAU). The authors from University of Warsaw acknowledge the support of National Science Centre of the Polish Ministry of Science and Higher Education, Grant No. 2011/01/B/ST2/02476

---

[1] M. Keim *et al.*, Nucl. Phys. A **586**, 219 (1995).
[2] M. R. Mumpower *et al.*, Astrophys. J. **752**, 117 (2012).
[3] M. Madurga *et al.*, Phys. Rev. Lett. **109**, 112501 (2012).
[4] A. L. Nichols, in *Workshop on Nuclear Reaction Data and Nuclear Reactors, Trieste, Italy* (2002).
[5] G. Rudstam, Nucl. Sci. and Eng. **80**, 238 (1982).
[6] M. C. Brady and T. R. England, Nucl. Sci. and Eng. **103**, 129 (1989).
[7] G. Lhersonneau, A. Wohr, B. Pfeiffer, K.-L. Kratz, and the ISOLDE Collaboration, Phys. Rev. C **63**, 034316 (2001).
[8] K.-L. Kratz *et al.*, Z. Phys. A **330**, 229 (1988).
[9] D. W. Stracener, Nuc. Instr. and Meth. in Phys. Res. B **204**, 42 (2003).
[10] J. R. Beene *et al.*, J. Phys. G **38**, 024002 (2011).
[11] S. V. Ilyushkin *et al.*, Phys. Rev. C **80**, 054304 (2009).
[12] http://www.xia.com/.
[13] R. Grzywacz *et al.*, Nuc. Instr. and Meth. in Phys. Res. B **204**, 649 (2003).
[14] R. Grzywacz *et al.*, Nuc. Instr. and Meth. in Phys. Res. B **261**, 1103 (2007).
[15] P. F. Dubois, K. Hinsen, and J. Hugunin, Computers in Physics **10** (1996).
[16] http://cars9.uchicago.edu/software/python/lmfit/, "Least-squares minimization with constraints for python,".
[17] C. J. Bischof and W. L. T. Jr., Phys. Rev. C **15**, 1047 (1977).
[18] C. M. Baglin, Nucl. Data. Sheets **112**, 1163 (2011).
[19] M. Quinn *et al.*, Phys. Rev. C **85**, 035807 (2012).
[20] J. K. Hwang *et al.*, Phys. Rev. C **82**, 034308 (2010).
[21] C. M. Baglin, Nucl. Data. Sheets **91**, 423 (2000).
[22] T. Rząca-Urban *et al.*, Eur. Phys. J. A **9**, 165 (2000).
[23] K. Debertin and U. Schötzig, Nuc. Instr. and Meth. **158**, 471 (1979).
[24] M. Wang *et al.*, Chin. Phys. C **36**, 1603 (2012).
[25] T. Kawano *et al.*, J. Nucl. Sci. Technol. **47**, 462 (2010).
[26] M. B. Chadwick *et al.*, Nucl. Data Sheets **112**, 2887 (2011).
[27] B. Singh, J. L. Rodriguez, S. S. M. Wong, and J. K. Tuli, Nucl. Data Sheets **84**, 487 (1998).
[28] K.-L. Kratz *et al.*, Z. Phys. A **312**, 43 (1983).
[29] K. Nakayama, Phys. Lett. B **114**, 217 (1982).
[30] K. Takahashi and M. Yamada, Prog. Theor. Phys. **41**, 1470 (1969).
[31] G. C. Carlson *et al.*, Nucl. Phys. A **125**, 267 (1969).
[32] M. Asghar *et al.*, Nucl. Phys. A **247**, 359 (1975).
[33] G. Rudstam and E. Lund, Phys. Rev. C **13**, 321 (1976).
[34] P. Patzelt and G. Herrmann, in *Proceedings of Symposium on Physics and Chemistry of Fission*, Vol. II (1965) p. 243.
[35] S. Amiel *et al.*, Phys. Rev. C **5**, 270 (1972).
[36] J. W. L. Talbert, A. Tucker, and G. Day, Phys. Rev. **177**, 1805 (1969).
[37] U. C. Bergmann *et al.*, Nucl. Phys. A **714**, 21 (2003).
[38] T. Mehren *et al.*, Phys. Rev. Lett. **77**, 458 (1996).
[39] G. F. Grinyer *et al.*, Phys. Rev. C **76**, 025503 (2007).
[40] T. Tachibana, M. Yamada, and Y. Yoshida, Prog. Theo. Phys. **84**, 641 (1990).
[41] P. Möller, J. R. Nix, and K.-L. Kratz, At. Data and Nucl. Data Tables **66**, 131 (1997).
[42] P. Möller, B. Pfeiffer, and K.-L. Kratz, Phys. Rev. C **67**, 055802 (2003).
[43] I. N. Borzov, Phys. Rev. C **67**, 025802 (2003).
[44] E. A. McCutchan *et al.*, Phys. Rev. C **86**, 041305(R) (2012).
[45] R. Surman and J. Engel, Phys. Rev. C **64**, 035801 (2001).